Paper No.
3912

CORROSION 2014
Collaborate. Educate. Innovate. Mitigate.
March 9-13, 2014 • Henry B. Gonzalez Convention Center • San Antonio, Texas, U.S.A.

Environmentally Assisted Cracking of Ultra Strength Low Alloy Steel in Sour Environments

M. Ziomek-Moroz
U.S. Department of Energy,
National Energy Technology Laboratory

1450 Queen Avenue SW
Albany, OR 97321
USA

J.A. Hawk
U.S. Department of Energy,
National Energy Technology Laboratory

1450 Queen Avenue SW
Albany, OR 97321
USA

R. Thodla
DNV, Columbus

5777Frantz Road
Dublin, OH 43301
USA

F. Gui
DNV, Columbus

5777Frantz Road
Dublin, OH 43301
USA

ABSTRACT

Catastrophic failures of drill pipes are a major concern in HPHT drilling environments. The National Energy Technology Laboratory, U.S. Department of Energy and DNV, Columbus are investigating mechanisms of crack propagation in ultra-high strength low alloy (UHSLA) martensitic steel drill pipe under cyclic stress as functions of pH, H_2S concentration and temperature in simulated production fluids. These fluids are deaerated 5% NaCl solution buffered with $NaHCO_3/Na_2CO_3$ or CO_2 in contact with 0.83 kPa H_2S. Microscopic investigations of the pre-cracked sample surfaces after corrosion fatigue tests revealed the presence of additional cracks that had propagated in the bulk material in neutral pH solution at 20°C. This paper discusses effects of the production fluid temperature on susceptibility of the UHSLA steel to environmentally assisted cracking. Post-corrosion fatigue surface characterization methods, such as optical and scanning electron microscopy, were used in this study.

Key words: Ultra-high strength low alloy steel, sour environments, corrosion fatigue

INTRODUCTION

Literature data indicate that approximately 20% of the drill pipe failures are caused by corrosion fatigue.[1] With the application of balanced pressure drilling technology, H_2S invades more easily into drilling fluids and with the use of high-strength drill pipe in deep and ultra-deep wells, the corrosion fatigue becomes more pronounced.[2]

©2014 by NACE International.
Requests for permission to publish this manuscript in any form, in part or in whole, must be in writing to
NACE International, Publications Division, 1440 South Creek Drive, Houston, Texas 77084.
The material presented and the views expressed in this paper are solely those of the author(s) and are not necessarily endorsed by the Association.

Taking into account that carbon-manganese steels are the most economic material for construction of pipelines, there has been a significant amount research performed on corrosion fatigue of this material in H_2S-containg environments, also called sour environments. The main effect of H_2S on steels is an observed increase in fatigue crack growth rate (FCGR), particularly when H_2S concentration is increased in simulated production fluids. [3-7]

The effect of low stress intensity range (ΔK) values leads to less increase in the FCGR over air values at comparable ΔK levels. Another important interaction effect of sour environments on FGCR is with the load cycle frequency. Literature data show that FCGR increases with decreasing frequency.[8-10] If the FCGR is influenced through a reaction controlled process, a plateau may be observed at low frequencies. If FCGR is controlled by a diffusion process, the plateau may be observed at higher frequencies.[11]

However, there is little available data for ultrahigh-strength low alloy steels needed for ultra deep drilling (UDD) operations. This paper discusses the effect for environmental variables on fatigue crack propagation in ultra high-strength steel in sour production fluid.

EXPERIMENTAL PROCEDURES

Crack growth rate experiments were performed using a ½T compact tension (CT) specimen that was machined from a 12.54 mm thick UHSLA steel drill pipe in the L-C orientation as shown schematically in Figure 1 with the notch running through thickness of the pipe.[12] The chemical composition and mechanical properties of the UHSLA steel pipe are shown Table 1 and Table 2, respectively.

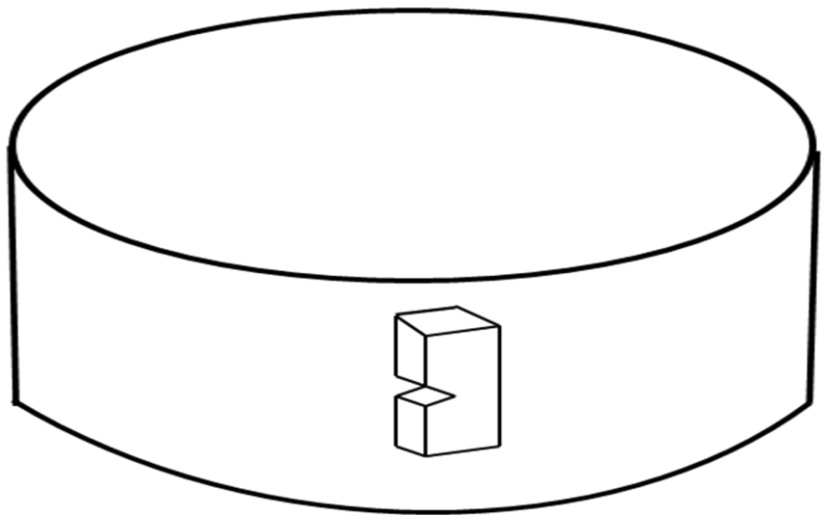

Figure 1: Scheme of L-C notch orientation in hollow or cylinder.

Table 1

Chemical Composition [wt%] of Chemical Composition [wt%] of UHSLA Steel

Fe	Cr	Mn	Mo	Al	Ni	Cu	Nb	S, N	P, B	C
Bal	0.79	0.88	0.67	0.03	0.81	0.19	0.02	0.007	<0.005	0.27

©2014 by NACE International.
Requests for permission to publish this manuscript in any form, in part or in whole, must be in writing to
NACE International, Publications Division, 1440 South Creek Drive, Houston, Texas 77084.
The material presented and the views expressed in this paper are solely those of the author(s) and are not necessarily endorsed by the Association.

Table 2

Mechanical Properties of UHSLA Steel

Ultimate Tensile Stress [MPa]	Yield Stress [MPa]	Elongation [%]	Hardness [R_c]
1278	1183	23.7	40.1

High strength low alloy steels attain high yield strength through the development of martensite. Figure 2 shows the typical martensitic microstructure developed in these steels for a UD-165 specimen polished to 0.05 µm finish and then chemically etched with 2% HNO_3 in C_2H_5OH.

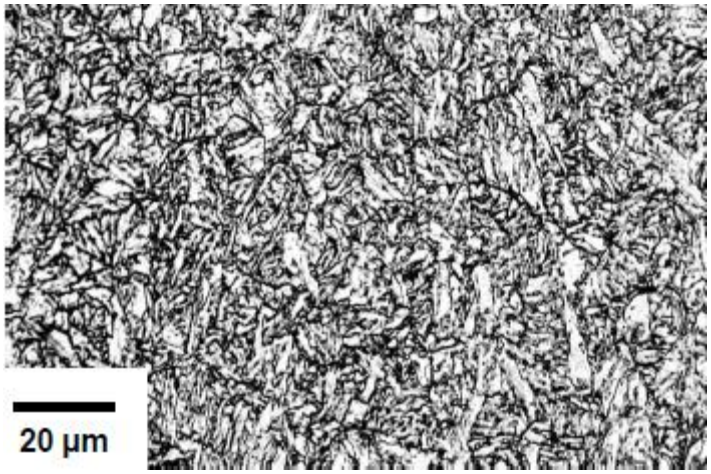

Figure 2: Microstructure of UHSLA steel.

Figure 3 shows the schematic representation of the experimental system used to determine FCGR during frequency scans.

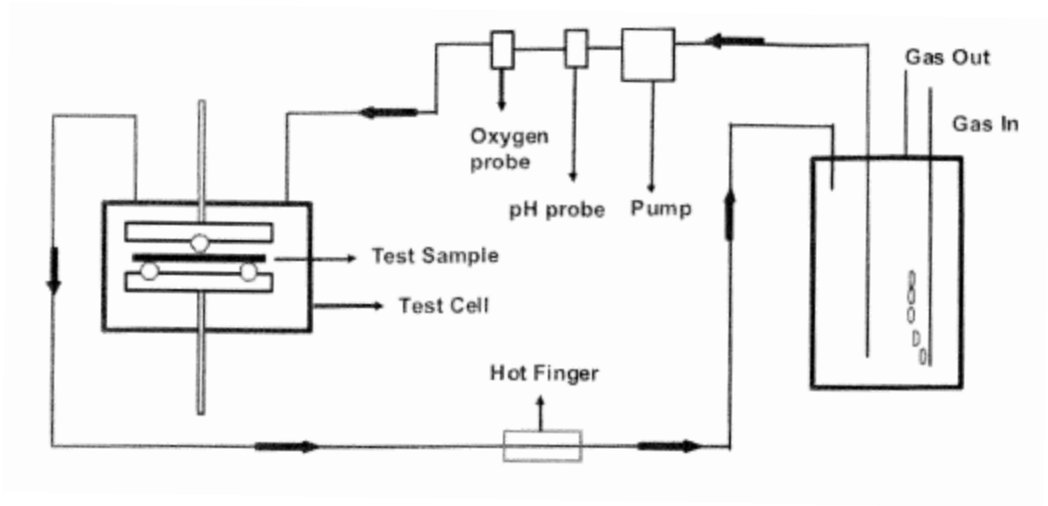

Figure 3: Scheme of experimental setup.

©2014 by NACE International.
Requests for permission to publish this manuscript in any form, in part or in whole, must be in writing to
NACE International, Publications Division, 1440 South Creek Drive, Houston, Texas 77084.
The material presented and the views expressed in this paper are solely those of the author(s) and are not necessarily endorsed by the Association.

The four liter autoclave is made of nickel-based superalloy and is connected to a 15 liter reservoir using a re-circulating loop. Configuration of the system in this manner prevented iron contamination of the solution. To further prevent electrolyte contamination, a hot finger was installed in the loop to deposit iron from the solution. The re-circulating loop was equipped with a pH meter and an oxygen sensor to measure the values of pH and oxygen during the experiment.

The autoclave was purged with high purity nitrogen prior to testing, i.e., prior to moving the solution through the system. To simulate a sour production fluid at pH = 7, $CO_2/NaHCO_3$ was used as a buffer. In order to prepare this solution, the 5% NaCl solution was made in the reservoir and then deaerated with nitrogen before saturating with CO_2. When the oxygen level in the solution was confirmed to be below 1 ppb using an oxygen probe, the N_2 gas flow was switched to the CO_2 gas. When $Na_2CO_3/NaHCO_3$ equilibrium was established, the pH was measured. Subsequently, a gas mixture of H_2S and N_2 was introduced into the solution. Once the partial pressure of H_2S reached 0.83 kPa (i.e., p_{H2S} = 0.83 kPa), the solution was re-circulated through the autoclave. Solution pH (i.e., 7 in this case) was maintained by keeping $CO_2/NaHCO_3$ equilibrated. To simulate a sour production fluid with pH values of 9 and 12, the test solution was deaerated with 5% NaCl buffered with $Na_2CO_3/NaHCO_3$ and in contact with H_2S. The partial pressure of H_2S (i.e., p_{H2S}) was 0.83 kPa and the pH of the solution was adjusted using NaOH to 9 or 12 at 20°C. The pH of 9 or 12 was maintained by using $Na_2CO_3/NaHCO_3$ equilibrium. All experiments were carried out at a pressure of 101.325 kPa.

Each ½T CT specimen was immersed in the test solution for three days prior to performing the frequency controlled FCGR experiments. Crack grow rate (CGR) was determined at a constant ΔK of 31.5 MPa√m with the stress intensity ratio (R) set at 0.13. Subsequent CGR experiments were performed as a function of frequency. The frequency was scanned from high to low, i.e., from 3 to 0.003 Hz, in order to establish the growing crack so that environmentally assisted CGR would be fully realized. All experiments were performed using servo-hydraulic mechanical test frames, and the crack growth rate was measured using direct current potential drop method.

Before each test, the specimen surfaces were wet polished using 800 grit SiC paper. Afterwards, the ½T CT specimens were cleaned in acetone in an ultrasonic bath for 30 minutes and then rinsed in isopropanol followed by distilled water. The test specimens were then warm air dried and placed in the autoclave. Once sealed inside the autoclave, the chamber was purged with N_2. When the solution reached the desired test conditions in the reservoir, it was introduced into the autoclave for the 72 hour stabilization period prior to starting the frequency scan.

After the CGR test was completed, the general features of the broad face of the specimen surface and the specific topography of the crack where it intersected that surface with respect to the corroded surface was investigated using scanning electron microscopy (SEM). The chemical identification of specific areas and specific features of interest were determined using energy dispersive X-ray spectroscopy (EDXS). Sulfur identification was obtained using wavelength dispersive X-ray spectroscopy (WDXS). Upon completion of these preliminary surface investigations, the broad surface of the specimen was polished for optical and SEM investigations to determine crack morphologies and their propagation modes. After this examination was completed, each ½T CT specimen was then broken open after immersion in liquid nitrogen, and the plane of the crack surface examined to determine changes in the morphology and elemental distribution within the plane of the growing crack.

RESULTS AND DISCUSSION

Fatigue Crack Growth Rate Model

Wei and Gangloff[11] proposed models for corrosion fatigue crack propagation based on understanding the processes taking place at the crack tip. The processes that are involved in the environmental enhancement of the crack growth in the high-strength carbon steels by H_2S in contact with aqueous environments are illustrated in schematically in Figure 4.

©2014 by NACE International.
Requests for permission to publish this manuscript in any form, in part or in whole, must be in writing to
NACE International, Publications Division, 1440 South Creek Drive, Houston, Texas 77084.
The material presented and the views expressed in this paper are solely those of the author(s) and are not necessarily endorsed by the Association.

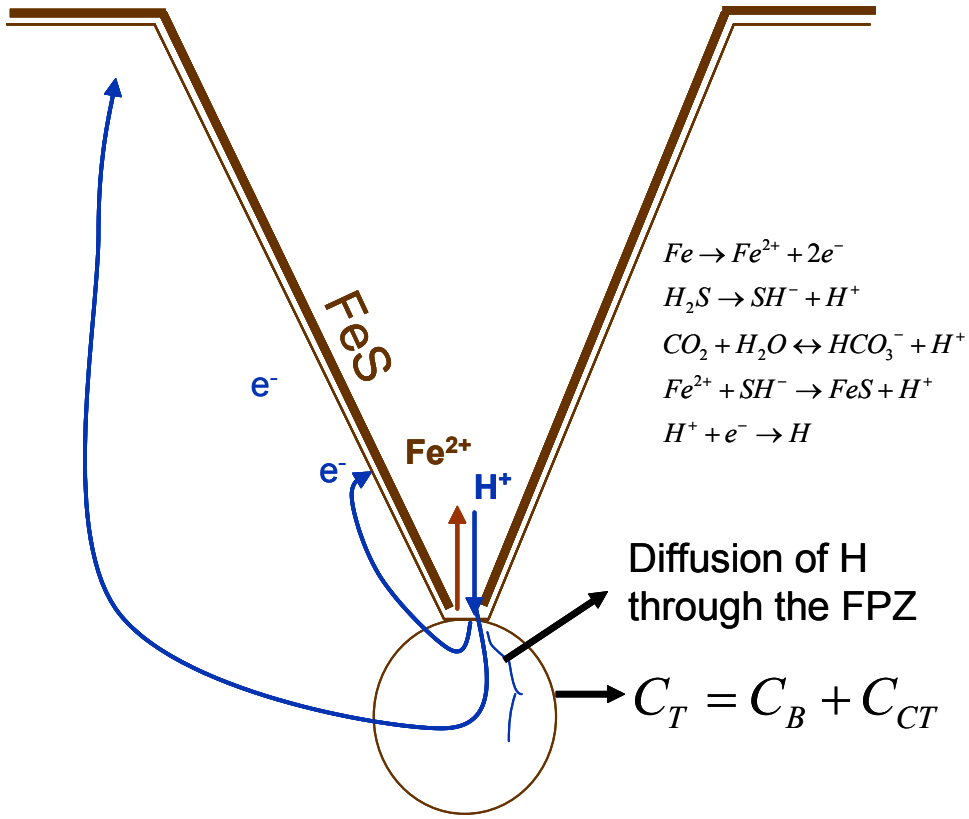

Figure 4: Schematic model of fatigue crack propagation for high strength carbon steel in aqueous H_2S. C_T is the total hydrogen in the crack tip, C_B is the hydrogen concentration from the bulk charging, C_{CT} is the hydrogen charged into the fracture.

The hydrogen generation reaction leads to adsorption, followed by absorption of hydrogen atoms in the metal. The absorbed hydrogen typically diffuses to the fracture process zone and causes embrittlement. It is worth noting that H_2S strongly enhances the absorption of hydrogen atoms by preventing their recombination into H_2. Also, non-dissociated H_2S molecules can produce H atoms and HS^- through the cathodic reaction, thereby generating more diffusible H that may further enhance metal degradation. This study is in progress.

The possible rate controlling steps in the hydrogen-related fatigue process may be related to the diffusion of hydrogen through the fracture process zone through surface reactions generating hydrogen, and/or stress corrosion cracking controlled growth. If the fatigue crack growth rate (da/dN) is controlled by the rate of hydrogen diffusion, then the experimental evidence for this model would be a linear relationship between logarithms of (da/dN) and frequency with a gradient of -0.5 (equation (1):

$$\log(da/dN) = -0.5\log f + \log A^- \quad (1)$$

In Equation (1) f is the frequency and A is proportional to hydrogen diffusion coefficient. The experimental results reported herein focus on determining the crack growth rate–frequency relationship.

Figure 5 shows the results of the FCGR experiments as a function frequency for pH values of 7, 9, and 12 in the sour solutions at 20°C.

©2014 by NACE International.
Requests for permission to publish this manuscript in any form, in part or in whole, must be in writing to
NACE International, Publications Division, 1440 South Creek Drive, Houston, Texas 77084.
The material presented and the views expressed in this paper are solely those of the author(s) and are not necessarily endorsed by the Association.

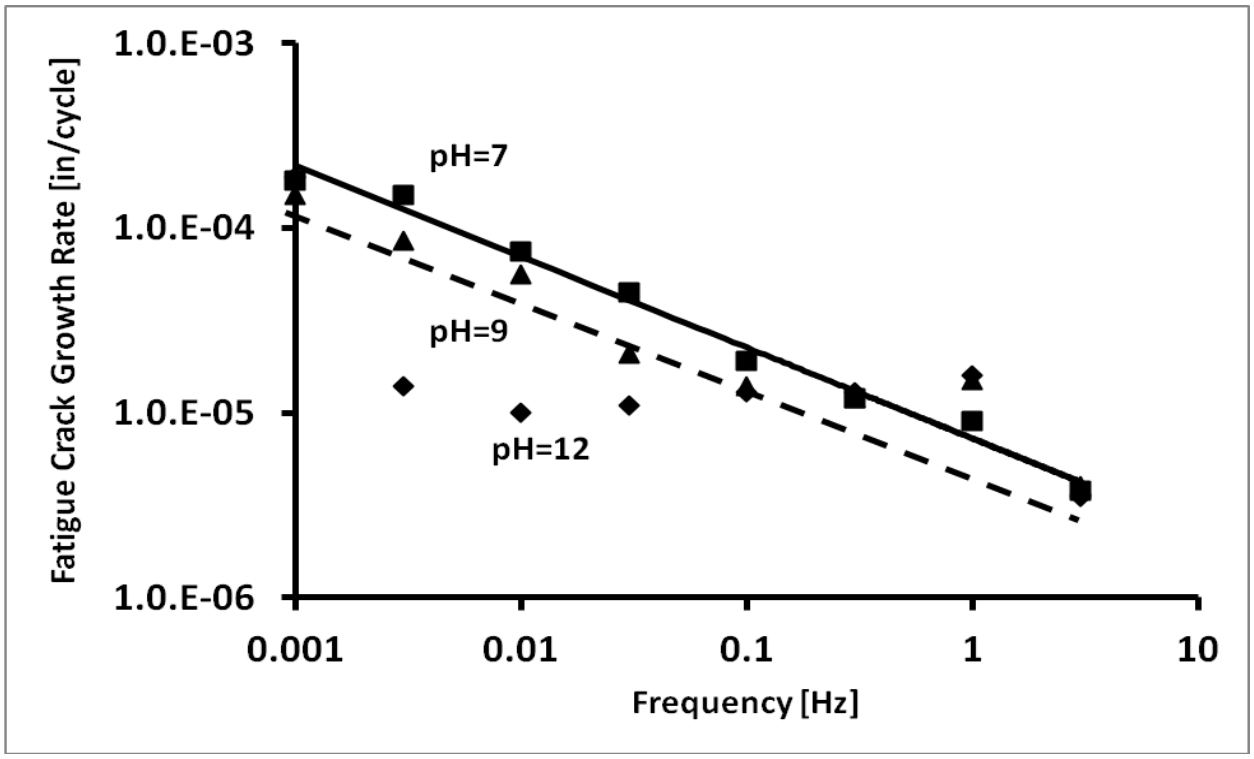

Figure 5: FCGR as a function of frequency for UHSLA steel 5%NaCl/$NaHCO_3$/CO_2/p_{H2S} = 0.83 kPa, pH=7 and 5%NaCl/$NaHCO_3$/Na_2CO_2/p_{H2S} = 0.83 kPa, pH=9 and 12, at 20°C.

For the experiments conducted at pH 7 and 9, the FCGR increases with decreasing frequency. The lines on the graph represent the fit to data using [Eq. 1]. The slope of each line is approximately -0.5, indicating FCGR is controlled by the rate of hydrogen diffusion in the crack tip zone.

However, with increase of pH to 12, the FCGR does not show the same linear dependence on frequency as observed for those solutions where the pH was 7 and 9. The lowest FCGR value, i.e., 3.5×10^{-6} in/cycle, occurs at 3 Hz. The highest FCGR occurred at 0.003 Hz and was measured at 1.4×10^{-5} in/cycle.

This change in CGR could be a result of the higher pH environment resulting in low corrosion rates, and thus, very small quantities of hydrogen entering the alloy. The presence of the CGR plateau may possibly indicate that corrosion products form near the growing crack, forming a plug that enhances crack closure. The applicability of Wei and Gangloff's FCGR model, based on the role of hydrogen kinetics at the crack tip of the UHSLA steel, is verified by the SEM study.

Figure 6 shows an SEM micrograph of near the crack tip area after FCGR testing in the pH = 12 solution.

©2014 by NACE International.
Requests for permission to publish this manuscript in any form, in part or in whole, must be in writing to
NACE International, Publications Division, 1440 South Creek Drive, Houston, Texas 77084.
The material presented and the views expressed in this paper are solely those of the author(s) and are not necessarily endorsed by the Association.

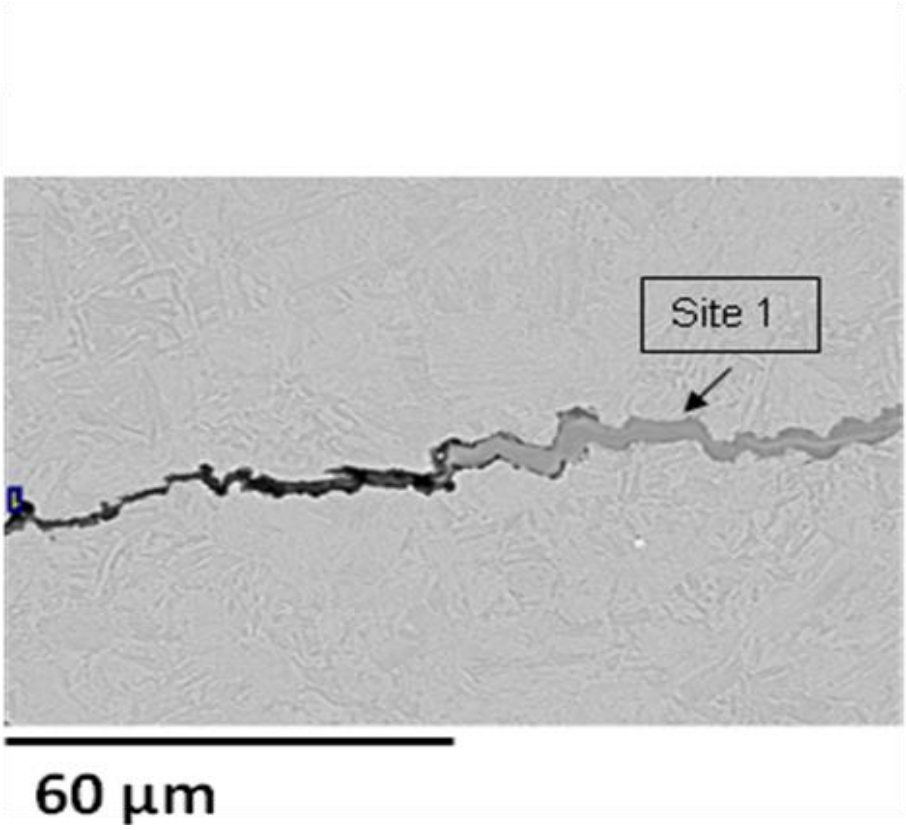

Figure 6: Backscattered SEM images of the polished surface after cyclic stress testing in 5% NaCl/$NaHCO_3$/Na_2CO_3/ p_{H2S} = 0.83 kPa, pH=12, at 20°C showing crack filled with (Fe, S)-rich corrosion products near the crack tip.

Inspection of the region containing the crack revealed the presence of corrosion product near the crack tip. The corrosion product is rich in Fe and S, based on analysis of the x-ray maps (not shown). Also, EDX and WDX analyses for S in Site 1 detected 52 at% Fe with 46 at% S. This result supports the FCGR-frequency results (Figure 5) that indicated possible plug formation, and therefore, limited access of hydrogen to the growing crack at the tip.

Figure 7 shows an SEM image of one side of the fatigue sample that failed catastrophically after FCGR testing in the pH = 7 solution.

In this case, inspection of the fracture surface indicated a brittle-type failure mechanism. Beside the main fatigue crack, small secondary cracks were observed on the polished surface,

©2014 by NACE International.
Requests for permission to publish this manuscript in any form, in part or in whole, must be in writing to
NACE International, Publications Division, 1440 South Creek Drive, Houston, Texas 77084.
The material presented and the views expressed in this paper are solely those of the author(s) and are not necessarily endorsed by the Association.

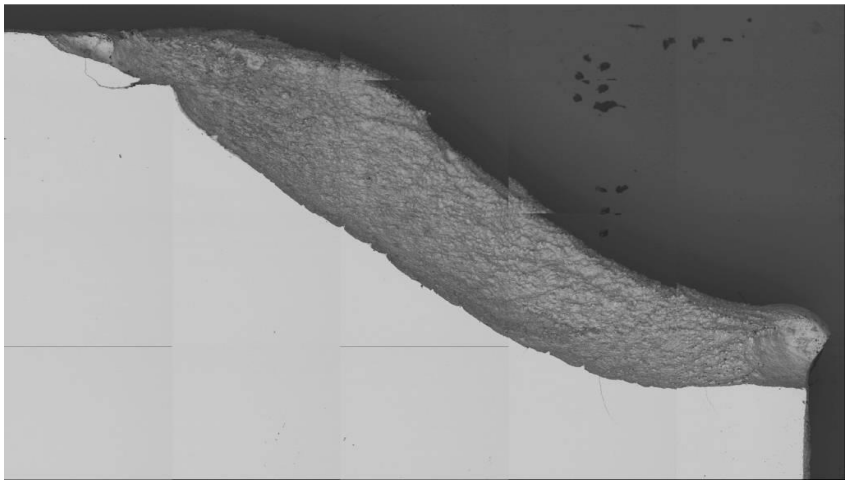

6 mm

Figure 7: Backscattered SEM fractograph of UHSLA steel after a fatigue test in NaCl/ CO_2/$NaHCO_3$/p_{H2S} = 0.83 kPa, pH=7 at 20°C, pH=7.

The X-ray map generated for S shows extensive S-rich regions. The original wavelength dispersive X-ray spectroscopy (WDXS) map indicated the S on the fracture surface using a false color. However, these regions did not show up very clearly when converted to black/white. In order to more accurately represent what was observed, the WDXS S map was overlaid onto the original (and identical) secondary electron image to enhance the overall contrast relative to those regions showing S. This is shown in Figure 8. Here the S-rich regions on the fracture are now "black" in color opposed to the "grey" appearance of the surface for those areas not showing S, in the notch and bulk metal. These results suggest that S and H species diffused throughout the specimen along preferential paths, causing embrittlement that resulted in catastrophic fracture. These results also confirm that in spite of the fact that Fe- and S-rich species formed along the H and S pathways, crack growth rate was still controlled by the hydrogen diffusion step.

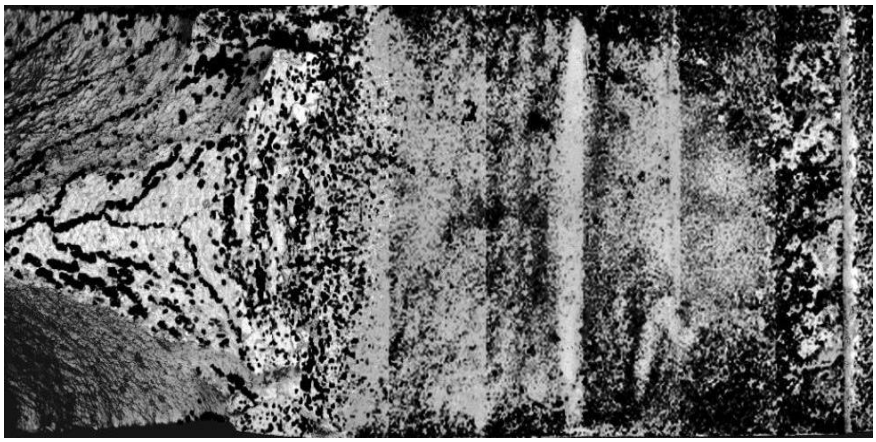

5 mm

Figure 8: X-ray map for S (black color) for UHSLA steel after a fatigue test in NaCl/ CO_2/$NaHCO_3$/p_{H2S} = 0.83 kPa, pH=7 at 20°C, pH=7. S-rich regions are marked in black color.

©2014 by NACE International.
Requests for permission to publish this manuscript in any form, in part or in whole, must be in writing to
NACE International, Publications Division, 1440 South Creek Drive, Houston, Texas 77084.
The material presented and the views expressed in this paper are solely those of the author(s) and are not necessarily endorsed by the Association.

Figure 9 shows an SEM micrograph of near the crack tip area after the FCGR testing in the pH=9.

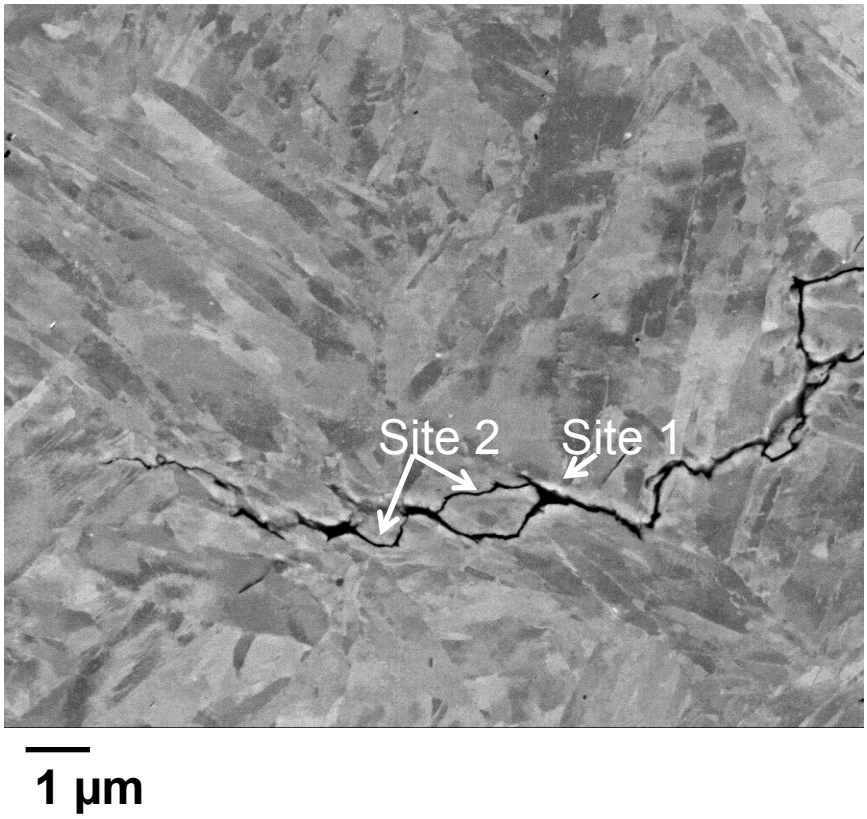

Figure 9: Backscattered SEM images of the polished surface after cyclic stress testing in 5% NaCl/$NaHCO_3$/Na_2CO_3/p_{H2S} = 0.83 kPa, pH=9, at 20°C showing crack morphology near the crack tip.

The crack propagates intergranulary and transgranulary. A few secondary cracks are observed near the crack tip. At site 1, EDX and WDX analyses detected the presence of 68 at% Fe and 17 at% S. Higher concentrations of Fe and S were detected in such pockets (Site 1 in Figure 9) compared to narrow cracks (Site 2 in Figure 9). Although Fe- and S-rich corrosion products were detected along the primary crack, it appears that they did not impede diffusion of hydrogen to the crack tip, so that FCGR was once again controlled by hydrogen diffusion.

CONCLUSIONS

- At pH values of 7 and 9 at 20°C, FCGR as function of frequency is linear with approximately a -0.5 gradient. This indicates that FCGR is controlled by hydrogen diffusion.

- At a pH value of 12 at 20°C, FCGR as function of frequency is non-linear indicating possible crack closure due to corrosion product formation at the crack tip.

- Scanning electron microscopy investigations of exposed specimens after FCGR experiments in pH = 7 and 9 solutions at 20°C revealed the presence of Fe and S-rich corrosion products that, in this case, did not serve as a diffusion barrier to S and H species at the crack tip.

- Scanning electron microscopy investigations of exposed specimens after FCGR experiments in pH = 12 solutions at 20°C revealed the presence of corrosion products at the crack tip, effectively plugging them.

©2014 by NACE International.
Requests for permission to publish this manuscript in any form, in part or in whole, must be in writing to
NACE International, Publications Division, 1440 South Creek Drive, Houston, Texas 77084.
The material presented and the views expressed in this paper are solely those of the author(s) and are not necessarily endorsed by the Association.

DISCLAIMER

This report was prepared as an account of work sponsored by an agency of the United States Government. Neither the United States Government nor any agency thereof, nor any of their employees, makes any warranty, express or implied, or assumes any legal liability or responsibility for the accuracy, completeness, or usefulness of any information, apparatus, product, or process disclosed, or represents that its use would not infringe privately owned rights. Reference herein to any specific commercial product, process, or service by trade name, trademark, manufacturer, or otherwise does not necessarily constitute or imply its endorsement, recommendation, or favoring by the United States Government or any agency thereof. The views and opinions of authors expressed herein do not necessarily state or reflect those of the United States Government or any agency thereof.

ACKNOWLEDGEMENTS

The authors would like to thank, Mr. Keith Collins for microscopic support.

REFERENCES

1. J. Jiashen, Z. Jingmao, “Increasing the Fatigue life of 40Cr Steel in Drilling Muds with Corrosion Inhibitors,” Corrosion, Vol. 49, p. 256.

2. F. Chaoyang, Z. Jiashen “Corrosion Fatigue Behavior of Carbon Steel in Drilling Fluids,” Corrosion, Vol. 54, p. 651.

3. S.E.Webster , I.M Austen and W.J. Rudd, “Fatigue, corrosion fatigue and stress corrosion of steels for offshore structures,” ECSC Report No. EUR 9460, ECSC Steel Publications, European

Commission, Brussels, 1985.

4. P. Bristoll and J. Roeleveld “Fatigue of offshore structures: effect of seawater on crack propagation in structural steel,” Proc. Conf. 'European Offshore Steels Research’, ECSC, 1978.

5. R.C. Eadie and K.E. Szklarz, “Fatigue initiation and crack closure of low alloy steels in sour brine environments,” Paper No. 610, Proc. Corrosion 99, NACE International, Houston, TX, 1999.

6. R.C. Eadie and K.E. Szklarz, “Fatigue crack propagation and fracture in sour dilute brine,” Paper No. 611, Proc. Corrosion 99, NACE International, Houston, TX, 1999.

7. S J Maddox, R J Pargeter and P Woollin, “Corrosion fatigue of welded C-Mn steel risers fordeepwater applications: a state of the art review’,” Paper OMAE2005-67499, 24th International Conference on Mechanics and Arctic Engineering (OMAE 2005) Halkidiki Greece, 12-16 June 2005.

8. J. Buitrago : “Effect of loading frequency on fatigue performance of risers in sour environment,” Paper 51641, Offshore Mechanics and Arctic Engineering Conference (OMAE 2004), Vol.III Materials Engineering, ASME, 2004.

9. R. I. Hammond and D. P. Baxter, “Corrosion fatigue of simulated C-Mn steel HAZ’s in sour produced fluids,” Paper OMAE 2008 - 57149, OMAE 2008 27th international Conference on Offshore Mechanics and Arctic Engineering, Estoril, Portugal, 15 – 20 June 2008.

©2014 by NACE International.
Requests for permission to publish this manuscript in any form, in part or in whole, must be in writing to
NACE International, Publications Division, 1440 South Creek Drive, Houston, Texas 77084.
The material presented and the views expressed in this paper are solely those of the author(s) and are not necessarily endorsed by the Association.

10. R. Thodla, F. Gui, R. Gordon, and J. Xia, “Corrosion Fatigue Performance of Girth Welded X65 Seamless Pipe for Flowline” NACE 2010, San Antonio.

11. R.P. Wei and R.P. Gangloff, "Environmentally Assisted Crack Growth in Structural Alloys: Perspectives and New Directions," *Fracture Mechanics: Perspectives and Directions (Twentieth Symposium), ASTM STP 1020,* R. P. Wei, and R. P. Gangloff,Eds.,American Society for Testing and Materials, Philadelphia, 1989, pp. 233-264].

12. ASTM E399-09 Standard Test Method for Linear-Elastic Plane-Strain Fracture Toughness K_{Ic} of Metallic Materials.

©2014 by NACE International.
Requests for permission to publish this manuscript in any form, in part or in whole, must be in writing to
NACE International, Publications Division, 1440 South Creek Drive, Houston, Texas 77084.
The material presented and the views expressed in this paper are solely those of the author(s) and are not necessarily endorsed by the Association.